FINITE SIZE EFFECTS IN LAYERED SUPERCONDUCTORS

Michielsen, K.; Schneider, T.; Raedt, H. De

Published in:
Zeitschrift für Physik. B: Condensed Matter

DOI:
10.1007/bf01387783

Publication date:
1991

Z. Phys. B – Condensed Matter 85, 15–21 (1991)

Condensed Zeitschrift für Physik B Matter

Finite size effects in layered superconductors

K. Michielsen[1,2], T. Schneider[1], and H. De Raedt[1,2]

[1] IBM Research Division, Zurich Research Laboratory, Säumerstrasse 4, CH-8803 Rüschlikon, Switzerland
[2] Institute for Theoretical Physics, University of Groningen, 9700 AV Groningen, The Netherlands

Received March 11, 1991; revised version May 13, 1991

We investigate the transition temperature of layered superconductors by considering a stack of L_z superconducting layers, separated by insulating material. We adopt a pairing Hamiltonian, invoke the variational principle and solve the resulting gap equations numerically. Our results confirm previous weak coupling and Ginzburg-Landau treatments and reveal a rise of T_c with L_z and saturation at the bulk transition temperature. Thus, the rise of T_c is traced back to a finite size effect, corresponding to a crossover from 2-*d* to 3-*d* superconductivity. The results also reveal a sizeable variation of the gap along the stack with pronounced variation at the ends.

I. Introduction

The mechanisms responsible for the behavior of the cuprate high temperature superconductors have remained elusive. Nevertheless, there is a generic property which they share with other layered superconductors, including superlattices, namely that the transition temperature exhibits a pronounced size effect. In fact, by considering a stack of L_z layers consisting of superconducting material, separated by insulating material, T_c was found to rise with L_z and to saturate at large L_z. Examples include Sn–SiO-, Al–AlO_2 superlattices [1], ultrathin $NbSe_2$-single crystals [2] and artificial YBCO/PrBCO superlattices [3–5].

This phenomenon appears to have close similarity to the rise of T_c in layered magnetic materials, where T_c increases with the number of magnetic layers L_z and saturates for large L_z values as well. In fact, mean field theory predicts for a layered square Ising model with nearest neighbor intra- and interlayer coupling J and J', respectively

$$T_c(L_z) = T_c(1)\left[1+\frac{|J'|}{|J|}\cos\left(\frac{\pi}{L_z+1}\right)\right], \tag{1}$$

where $T_c(1)$ is the transition temperature of the 2-*d* system. Thus, $T_c(1)$ rises from the 2-*d* value $T_c(1)$ to the 3-*d* bulk value for $L_z \to \infty$ [6]. This phenomenon is a size effect, corresponding to a crossover from 2-*d* to 3-*d* behavior, driven by the increasing value of the effective number of nearest neighbors. It is important to emphasize that the predicted rise of T_c is not an artifact of the mean field approximation or a pecularity of the Ising model [7–10]. The Heisenberg model exhibits similar behavior for any number of components (n) of the order parameter. For $n>1$, however, there is no long-range order below T_c for any finite L_z [11].

In this paper we investigate the variation of T_c and of the gap in layered superconductors within the framework of the model proposed in [6]. In doing so, we treat the pairing Hamiltonian by means of the variational principle. The gap equations are then solved numerically. These results complement the previous approximate treatments, using the Ginzburg-Landau approach, only valid close to T_c, or the weak coupling solution of the gap equation. Crucial ingredients of the model are an intralayer and interlayer pairing interaction of strength g_0 and g_3, respectively. The interlayer interaction g_3 couples the order parameters in adjacent layers in analogy to a stack of coupled two-dimensional xy-models. For finite interlayer single particle hopping and negligible g_3, the model reduces in its Ginzburg-Landau form to that proposed by Lawrence and Doniach [12]. In Sect. 2 we sketch the models and derive the associated gap equations by means of the variational principle. Their linearized versions are then used to determine the critical temperature. Since the interlayer single particle hopping matrix element is supposed to be small, we consider two models. One with finite and the other with vanishing interlayer hopping.

In Sect. 3 we present and discuss our numerical results for stacks consisting of L_z layers. For finite g_3, the results clearly reveal an initial increase of T_c with L_z and saturation for large L_z values. The essential features of this phenomenon agree remarkably well with the previous Ginzburg-Landau treatment and the weak coupling pre-

dictions [6]. The rise of T_c corresponds to a finite size effect, or equivalently, to a crossover from two to three-dimensional superconductivity. The numerical results also reveal that the rise of T_c with L_z is due exclusively to the interlayer coupling g_3. In fact, the presence of single particle hopping turns out to reduce T_c with increasing L_z. In contrast to the magnetic case (1), however, the increase of T_c is not simply given by the ratio of the inter- and intralayer coupling. Another interesting issue is the variation of the gap along the stack of L_z layers. The numerical results clearly point to a reduction of the zero temperature gap close to and at the free ends. Finally we discuss the differences resulting from taking free instead of periodic boundary conditions in the z-direction.

II. Model

To investigate the variation of T_c with the number of layers, we consider a model in which the pairing interaction includes an intralayer and an interlayer interaction. In a first step we neglect the interlayer single particle hopping. The system is assumed to be infinite in the xy-plane but finite along the z-direction. Accordingly we choose periodic boundary conditions in the planes and free ends in the z-direction.

II.1. Interlayer hopping excluded

We consider the Hamiltonian

$$\mathcal{H} = \mathcal{H}_1 + \mathcal{H}_2, \tag{2}$$

where

$$\mathcal{H}_1 = \sum_{\mathbf{k}, l, \sigma} (\tilde{\varepsilon}(\mathbf{k}) - \mu)\, c^+_{\mathbf{k}, l, \sigma} c_{\mathbf{k}, l, \sigma} \tag{3}$$

describes the quasi-particle band; l is the layer index, $\mathbf{k}$ is the wave vector in the xy-plane, σ is the spin index and μ is the chemical potential. For the quasiparticle band we adopt [13, 14]

$$\tilde{\varepsilon}(\mathbf{k}) = A[-2(\cos k_x a + \cos k_y a) + 4B \cos k_x a \cos k_y a], \tag{4}$$

where A is the nearest-neighbor and AB the next-nearest-neighbor hopping within the layers, respectively. Within the layers we assume a square lattice with lattice constant a. For the pairing interactions we assume

$$\mathcal{H}_2 = -g_0 \sum_{\mathbf{k}, l} n_{\mathbf{k}, l, \uparrow} n_{\mathbf{k}, l, \downarrow} - g_3 \sum_{\mathbf{k}, l} (c^+_{\mathbf{k}, l+1, \uparrow} c^+_{\mathbf{k}, l+1, \downarrow} c_{\mathbf{k}, l, \downarrow} c_{\mathbf{k}, l, \uparrow} + \text{c.c.}), \tag{5}$$

where $g_0 > 0$ is the strength of the intralayer coupling and g_3 is the strength of the recently proposed interlayer interaction [6]. In the Ginzburg-Landau formulation of the model, g_3 leads to a Heisenberg-type interaction of the order parameters in adjacent layers and in turn to a L_z dependence of T_c, reminiscent of magnetic systems (1).

To derive the gap equation we use the variational principle, which means that we minimize the free energy $\beta F = -\ln \mathrm{Tr} e^{-\beta H}$ with respect to a trial Hamiltonian $\mathcal{H}_0$. The inequality for F reads

$$F \leqq F_0 + \langle \mathcal{H} - \mathcal{H}_0 \rangle_0. \tag{6}$$

The trial Hamiltonian is given by

$$\mathcal{H}_0 = \mathcal{H}_1 + \sum_{\mathbf{k}, l} \Delta(\mathbf{k}, l)(c^+_{\mathbf{k}, l, \uparrow} c^+_{-\mathbf{k}, l, \downarrow} + \text{c.c.}), \tag{7}$$

where we have assumed that $\Delta(\mathbf{k}, l) = \Delta^*(\mathbf{k}, l)$. It is important to recognize that our choice of $\mathcal{H}_0$ is motivated by the observation that $\mathcal{H}_0$ can be diagonalized by a Bogoliubov transformation, due to the absence of interlayer hopping. Minimizing the right-hand side of (6) we obtain the real space gap equation

$$\Delta(\mathbf{k}, l) = g_0 f(l) + g_3[f(l+1) + f(l-1)], \tag{8}$$

where

$$f(l) = \frac{1}{L^2} \sum_{\mathbf{k}} \frac{\Delta(\mathbf{k}, l)}{2E(\mathbf{k}, l)} \tanh\left(\frac{\beta E(\mathbf{k}, l)}{2}\right), \tag{9}$$

and

$$E(\mathbf{k}, l) = \sqrt{\varepsilon^2(\mathbf{k}) + \Delta^2(\mathbf{k}, l)}, \tag{10}$$

$$\varepsilon(\mathbf{k}) = \tilde{\varepsilon}(\mathbf{k}) - \mu. \tag{11}$$

From (8) we see that $\Delta(\mathbf{k}, l)$ is independent of $\mathbf{k}$. Thus, we can henceforth drop the label $\mathbf{k}$. The chemical potential μ is fixed by the band filling

$$\rho = \frac{1}{L^2 L_z} \sum_{\mathbf{k}, l} \left[1 - \frac{\varepsilon(\mathbf{k})}{E(\mathbf{k}, l)} \tanh\left(\frac{\beta E(\mathbf{k}, l)}{2}\right)\right], \tag{12}$$

where L^2 is the number of sites in the xy-plane and L_z is the number of sites in the z-direction. The gap $\Delta(\mathbf{k}, l)$ and chemical potential μ are the solutions of the coupled equations (8) and (12) with lowest free energy. Linearization of the gap equation leads to the equation for T_c

$$\Delta(l) = g_0 f_c \Delta(l) + g_3 f_c(\Delta(l+1) + \Delta(l-1)) \tag{13}$$

with

$$f_c = \frac{1}{L^2} \sum_{\mathbf{k}} \frac{1}{2\varepsilon(\mathbf{k})} \tanh\left(\frac{\beta_c \varepsilon(\mathbf{k})}{2}\right). \tag{14}$$

Equation (13) leads to the following eigenvalue problem for T_c:

$$\det\begin{pmatrix} 1-g_0 f_c & -g_3 f_c & 0 & \dots & \dots & 0 \\ -g_3 f_c & 1-g_0 f_c & -g_3 f_c & 0 & \dots & 0 \\ 0 & -g_3 f_c & 1-g_0 f_c & \ddots & 0 & 0 \\ 0 & 0 & \ddots & \ddots & \ddots & 0 \\ 0 & \dots & 0 & \ddots & \ddots & -g_3 f_c \\ 0 & \dots & \dots & 0 & -g_3 f_c & 1-g_0 f_c \end{pmatrix}=0. \tag{15}$$

The critical temperature T_c is then given by the highest temperature for which

$$\prod_{q=1}^{L_z}\left[1-\left(g_0+2g_3\cos\frac{\pi q}{L_z+1}\right)f_c\right]=0, \tag{16}$$

i.e.

$$\left(g_0+2|g_3|\cos\frac{\pi}{L_z+1}\right)f_c=1. \tag{17}$$

At T_c the equation for μ reads

$$\rho=\frac{1}{L^2}\sum_{\mathbf{k}}\left(1-\tanh\left(\frac{\beta_c\varepsilon(\mathbf{k})}{2}\right)\right). \tag{18}$$

Thus T_c and μ are the solutions of the coupled equations (17) and (18). At this point it is important to recognize that even a repulsive interlayer coupling g_3 enhances T_c. This is due to the fact that the Hamiltonian (see (2), (3), (5)) remains unchanged if we let $g_3\to -g_3$ and $c^+_{\mathbf{k},2l,\sigma}\to\exp(i\pi/2)c^+_{\mathbf{k},2l,\sigma}$, i.e., by reversing the sign of g_3 and adjusting the phase of the electron wave function on even-numbered layers.

II.2. Interlayer hopping included

To clarify the effect of single particle interlayer hopping we next consider the Hamiltonian

$$\mathscr{H}=\mathscr{H}_1+\mathscr{H}_2, \tag{19}$$

where

$$\mathscr{H}_1=\sum_{\mathbf{k},l,\sigma}\left[\tilde{\varepsilon}(\mathbf{k})c^+_{\mathbf{k},l,\sigma}c_{\mathbf{k},l,\sigma}-t(c^+_{\mathbf{k},l,\sigma}c_{\mathbf{k},l+1,\sigma}+\text{c.c.})-\mu\right] \tag{20}$$

describes the quasiparticle band, including the interlayer hopping of strength t. For this band we adopt the tight binding expression [13, 14]

$$\tilde{\varepsilon}(\mathbf{k},k_z)=A[-2(\cos k_x a+\cos k_y a)+4B\cos k_x a\cos k_y a-2C\cos k_z s], \tag{21}$$

where a is the lattice constant of the square lattice within the layers and s the spacing between the layers. The nearest-neighbor hopping matrix element within the layers is denoted by $-2A$, the next-nearest-neighbor one within the layers by $4AB$, and that for nearest-neighbor hopping between the layers by $AC=t$. For the pairing interaction we use the intralayer and interlayer couplings given in (5). To obtain the gap equation we invoke again the variational principle. The trial Hamiltonian $\mathscr{H}_0$ is now given by

$$\mathscr{H}_0=\mathscr{H}_1+\sum_{\mathbf{k},q}\Delta(\mathbf{k},q)(c^+_{\mathbf{k},q,\uparrow}c^+_{-\mathbf{k},q,\downarrow}+\text{c.c.}), \tag{22}$$

where electrons with the same q-value are paired because of the absence of translational symmetry in the z-direction due to the free boundary conditions. In contrast to the model where the single particle interlayer hopping was not included, $\mathscr{H}_1$ has to be diagonalized by Fourier transformation. The gap equation (for a detailed derivation we refer to Appendix A) then reads

$$\Delta(q)=-\frac{g_0+2g_3}{L_z+1}\sum_{q'}f(q')-\left(g_0+2g_3\cos\frac{2\pi q}{L_z+1}\right)\cdot\left[\frac{f(q)+f(L_z+1-q)}{2(L_z+1)}\right], \tag{23}$$

where

$$f(q)=\frac{1}{L^2}\sum_{\mathbf{k}}\frac{\Delta(q)}{2E(\mathbf{k},q)}\tanh\left(\frac{\beta E(\mathbf{k},q)}{2}\right), \tag{24}$$

$$E(\mathbf{k},q)=\sqrt{\varepsilon^2(\mathbf{k},q)+\Delta^2(q)}, \tag{25}$$

$$\varepsilon(\mathbf{k},q)=\tilde{\varepsilon}(\mathbf{k},q)-\mu. \tag{26}$$

Here we used the fact that $\Delta(\mathbf{k},q)\equiv\Delta(q)$. The variational parameter $\Delta(q)$ and the chemical potential μ are the solutions of the coupled equations (23) and (12), subject to the condition that the free energy is minimal. The real space expression $\Delta(l,l')$ is then obtained by inverse Fourier transformation and reads

$$\Delta(l,l')=\frac{2}{L_z+1}\sum_q\sin\frac{\pi q l}{L_z+1}\sin\frac{\pi q l'}{L_z+1}\Delta(q). \tag{27}$$

In contrast to the model where the single particle hopping was neglected, the variational parameter now depends on two indices. The critical temperature T_c and the chemical potential μ are then obtained from the solution of the coupled equations

$$1=\frac{g_0+2g_3}{L_z+1}\sum_q \frac{f_c(q)}{1-\left(g_0+2g_3\cos\frac{2\pi q}{L_z+1}\right)[f_c(q)+f_c(L_z+1-q)]/2(L_z+1)} \tag{28}$$

and

$$\rho=\frac{1}{L^2L_z}\sum_{\mathbf{k},q}\left(1-\tanh\left(\frac{\beta_c\varepsilon(\mathbf{k},q)}{2}\right)\right), \tag{29}$$

whereby

$$f_c(q)=\frac{1}{L^2}\sum_{\mathbf{k}}\frac{1}{2\varepsilon(\mathbf{k},q)}\tanh\left(\frac{\beta_c\varepsilon(\mathbf{k},q)}{2}\right). \tag{30}$$

In the limit $L_z=1$ the equation for T_c reduces to

$$1=g_0 f_c, \tag{31}$$

where f_c is given by (14). For $L_z\to\infty$, the equation for T_c becomes identical to that for periodic boundary conditions along the z-direction and we recover for $C=0$ the $L_z\to\infty$ limit of (17).

III. Numerical results

III.1. Critical temperature

To investigate the influence of interlayer interaction g_3, interlayer hopping C and boundary conditions on the critical temperature, we solve the coupled nonlinear equations (17) and (18), and (28) and (29) by iteration. Guided by earlier work [14] we chose

$$A=1,\quad B=0.45,\quad C=0.2,$$
$$g_0=1,\quad g_3=0.225,\quad \rho=0.7 \tag{32}$$

as the reference set of parameter values. To mimic superlattices, consisting of a finite stack of layers, we adopt free boundary conditions in the z-direction. In the xy-plane we use $L=128$, which turned out to be sufficient to provide nearly L-independent results.

First we consider the size dependence of the critical temperature T_c, namely $T_c(L_z)$, in the absence of interlayer single particle hopping, and compare the results on the basis of the two different trial Hamiltonians (7) and (22). Results obtained from a numerical solution of the coupled Eqs. (17) and (18), and (28) and (29) are depicted in Fig. 1. For $L_z=1, 2$ both the real and the q-space approach yield the same results, but for $L_z>2$ the latter yields slightly lower T_c. The results for model (21) including interlayer hopping do not coincide at $C=0$ with those of (4), since we have used the trial Hamiltonian (22) to calculate the properties of model (21) and the trial Hamiltonian (7) to calculate those of (4). We also included the results for $g_3=0$, i.e. without interlayer interaction. Here, as it should be $T_c(L_z)=T_c(1)$. For $g_3>0$, however, T_c rises considerably as the number of layers increases from $L_z=1$ to $L_z\approx 6$ where it approaches the value of the infinite system $L_z\to\infty$. As shown in Fig. 2, the rise of T_c is fully controlled by the magnitude of g_3. In fact, for $g_3=0$, there is no rise in T_c. This behavior can be understood in terms of the Ginzburg-Landau treatment of the problem. The result is [6]

$$T_c(L_z)=T_c(1)\left[1+a(0)\cos\left(\frac{\pi}{L_z+1}\right)\right], \tag{33}$$

with $a(0)=2|\lambda_3|/\lambda_0^2$ and $\lambda_n=g_nN(0)$, where $N(0)$ is the density of states at the Fermi level. From the results shown in Fig. 2 the ratio of the $a(0)$ values is 2.1, which is close to 2, the ratio of the corresponding g_3 values. Thus, our numerical results confirm the Ginzburg-Landau expression for T_c. Comparing Eqs. (1) and (33) it also becomes clear that the dependence of T_c on the intra-interlayer couplings differs substantially for magnetic and superconducting superlattices. The actual g_3 values used in Figs. 1 and 2 have been chosen to obtain a rise of $T_c(L_z)$ close to that observed in YBCO/PrBCO superlattices [3–5].

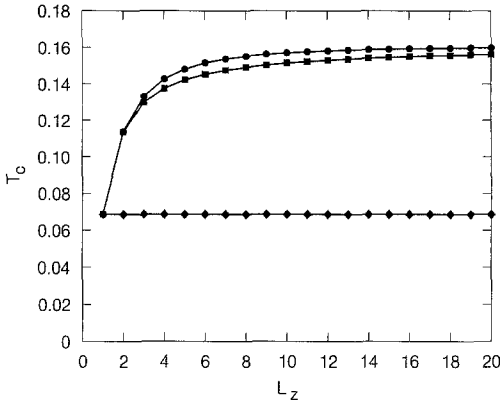

Fig. 1. Dependence of T_c on the number of layers L_z; ●: T_c calculated from (17) and (18); ■: T_c calculated from (28) and (29) with $C=0$; ◆: T_c calculated from (17) and (18) for $g_3=0$ and (28) and (29) for $C=g_3=0$

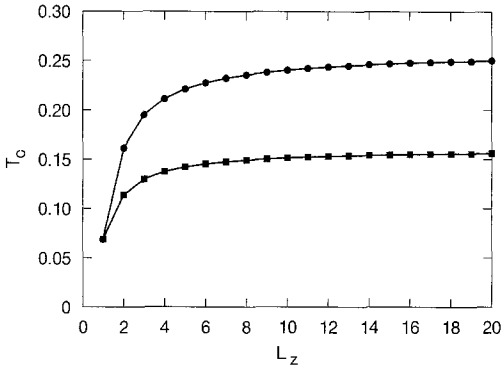

Fig. 2. Critical temperature T_c given by (28) and (29) with $C=0$, versus the number of layers for different values of g_3; ■: $g_3=0.225$; ●: $g_3=0.45$

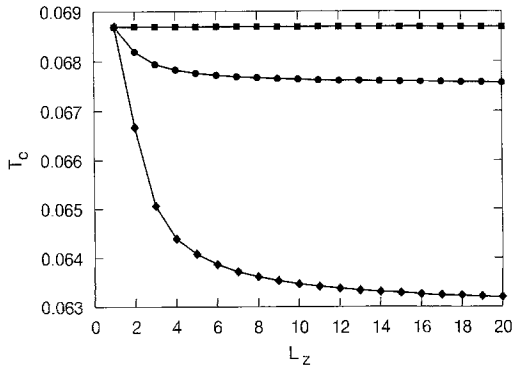

Fig. 3. Critical temperature T_c as a function of the number of layers L_z for various values of the interlayer hopping C, as calculated from (28) and (29), for $g_3=0$; ■: $C=0$; ●: $C=0.1$; ◆: $C=0.2$

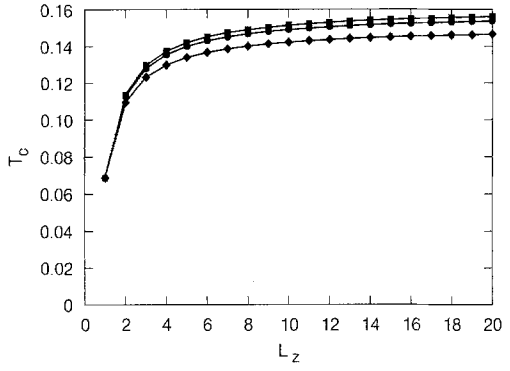

Fig. 4. Critical temperature T_c as a function of the number of layers L_z for various values of the interlayer hopping C, as calculated from (28) and (29), for $g_3=0.225$; ■: $C=0$; ●: $C=0.1$; ◆: $C=0.2$

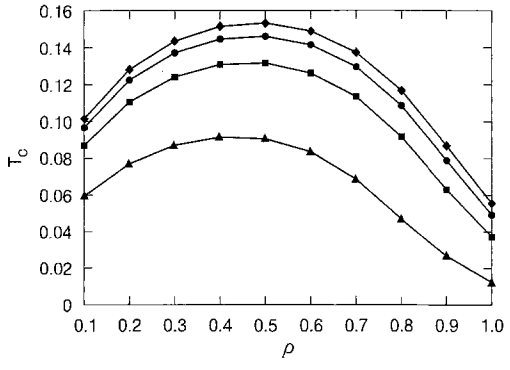

Fig. 5. Critical temperature T_c, obtained from (28) and (29) with $C=0$, versus band filling ρ for different values of L_z; ▲: $L_z=1$; ■: $L_z=2$; ●: $L_z=3$; ◆: $L_z=4$

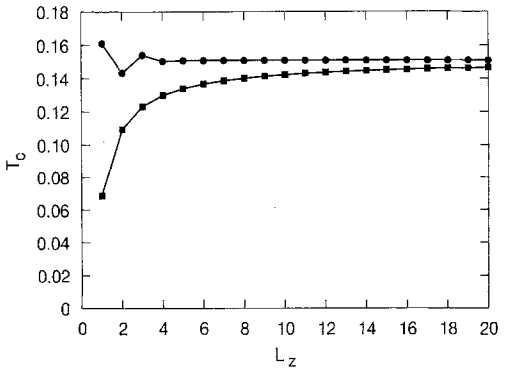

Fig. 6. Effect of the boundary conditions in the z-direction on T_c, given by (28) and (29), versus the number of layers L_z; ■: free boundary conditions; ●: periodic boundary conditions

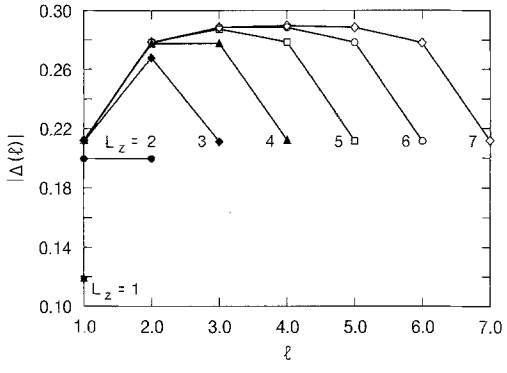

Fig. 7. Order parameter $|\Delta(l)|$ given by (8) and (12) versus layer index l for different values of L_z

To explore the effect of a non-zero interlayer hopping, calculations have also been performed for $g_3=0$ and various C values. Typical results are depicted in Fig. 3, revealing that T_c decreases with rising C. This reduction mirrors the variation of the density of states with C. In fact, for fixed $\rho=0.7$, the density of states at the Fermi level decreases with increasing C. The combined effect of non-zero g_3 and C is shown in Fig. 4. Here we plotted $T_c(L_z)$ for $C=0$, $C=0.1$ and $C=0.2$. In view of the results discussed above we expect T_c to rise with g_3 and to decrease with C as the stack becomes thicker. This is clearly borne out by the results shown in Fig. 4. Figure 5 shows typical results for T_c for various band fillings ρ and for L_z ranging from 1 to 4 layers. The critical temperature T_c reaches a maximum for $\rho\approx 1/2$, i.e. one quarter of a filled band. In going from 1 to 4 layers the relative enhancement of T_c is largest for $\rho\approx 1$.

In Fig. 6 we compare the results of free and periodic boundary conditions for the standard set of model parameters (32). Apparently, for a small number of layers periodic boundary conditions lead to a non-monotonic L_z dependence of T_c, while free boundaries lead to a monotonic rise. Clearly, describing a superlattice of finite thickness requires free boundary conditions.

III.2. Gap equation at $T=0$

To investigate the variation of the order parameter $\Delta(l)$ along a stack of L_z layers, we solved Eqs. (8)–(12) numerically in the limit $\beta\to\infty$ ($T=0$). Because the sign of g_3 only affects the phase of the order parameter, we depicted the absolute value of $|\Delta(l)|$ in Fig. 7. Apparently, $|\Delta(l)|$ is suppressed at the ends of the stack and reaches its maximum value within a few lattice constants.

Our results for the $T=0$ gap at the stack boundary exemplify the weakening of the pair potential at a surface due to the short coherence length [15]. Indeed, from

Table 1. Numerical estimates for the gap $\Delta(l)$ and T_c for $L_z=1, \ldots, 5$ for the set of parameters given in (33). Energies are in units of A (33)

L_z	$\Delta(1)$	$\Delta(2)$	$\Delta(3)$	k_BT_c	$2\Delta(1)/k_BT_c$	$2\Delta(2)/k_BT_c$	$2\Delta(3)/k_BT_c$
1	0.12			0.070	3.43		
2	0.20			0.115	3.48		
3	0.21	0.27		0.130	3.23	4.15	
4	0.21	0.28		0.140	3.00	4.00	
5	0.21	0.28	0.29	0.142	2.96	3.94	4.08

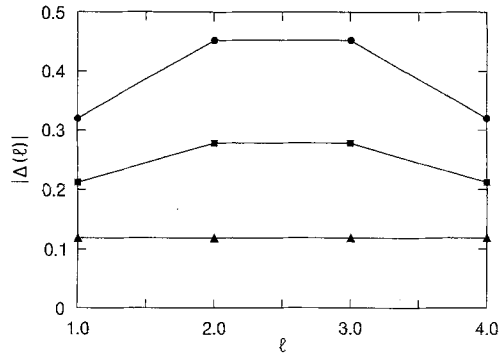

Fig. 8. Order parameter $|\Delta(l)|$, given by (8) and (12), versus the layer index l for different values of g_3 and $L_z=4$; ▲: $g_3=0$; ■: $g_3=0.225$; ●: $g_3=0.45$

Fig. 7 one learns that $|\Delta(l)|$ changes abruptly from its bulk value to its surface value over a distance of one lattice spacing, whereas a calculation of the pair correlation function reveals that the correlation length is much less than the interlayer spacing s. This reduction of the order parameter at surfaces affects many properties [15]. Estimates for the gap values, as shown in Fig. 7, are summarized in Table 1, together with the ratio $2|\Delta(l)|/k_BT_c$. For bulk superconductors and in the weak coupling BCS-theory the ratio is 3.54, while in the present case the interlayer coupling g_3 leads to variations of the gap and in turn of this ratio. Since for $L_z>2$ there is no longer only one gap, the density of states is a superposition of square-root singularities. This in turn should affect single-particle tunneling experiments as they probe the density of states directly.

The effect of the strength of g_3 on $\Delta(l)$ is illustrated in Fig. 8 for $L_z=4$. As $|g_3|$ increases, both the magnitude of the order parameter $\Delta(l)$ and the difference between the surface and bulk value are seen to increase as well. To explore the effect of interlayer hopping on the behavior of the order parameter we also solved Eqs. (12) and (23)–(26) and invoked Eq. (27) to transform the q-space data into real space. The results (not shown) reveal that there are only small differences between the real and q-space formulation. An exception is the increase in magnitude of the order parameters $|\Delta(l, l')|$ as a function of the distance to the surface, which is much smaller than predicted by the real-space approach. In the absence of single particle interlayer hopping this variation turns out to be more pronounced.

IV. Discussion

We have calculated T_c and the gap at $T=0$ for finite stacks of superconducting layers. The experimentally observed rise of T_c with the number of layers can be accounted for by including a particular type of interlayer pairing interaction (g_3), which may be repulsive or attractive. We also demonstrated that incorporating interlayer hopping reduces the critical temperature.

To investigate the possibility that interactions of different type can lead to effects similar to those due to g_3, we have repeated the above analysis for the two other types of nearest-neighbor interlayer interactions (g_1 and g_2), whose physical origin is discussed in [16, 17]. The influence of g_1 on T_c of an infinite stack has been examined earlier [18], and was found to be of minor importance for realistic values of $|g_1|$ (i.e. $|g_1/g_0|\ll 1$). A proper treatment of the boundary effects does not alter this conclusion. Furthermore, a pairing interaction of the type

$$\sum_{\mathbf{k},l,m}(g_{lm}c^+_{\mathbf{k},l,\uparrow}c^+_{\mathbf{k},m,\downarrow}c_{\mathbf{k},l,\downarrow}c_{\mathbf{k},l,\uparrow}+\text{c.c.})$$
$$+\sum_{\mathbf{k},l,m}(g_{lm}c^+_{\mathbf{k},m,\uparrow}c^+_{\mathbf{k},l,\downarrow}c_{\mathbf{k},l,\downarrow}c_{\mathbf{k},l,\uparrow}+\text{c.c.}),$$

where $g_{lm}=g_2(\delta_{l,m-1}+\delta_{l,m+1})$, leads to an increase of g_0 and hence to a rise of T_c, but independently of the number of layers. We have therefore established that of all possible nearest-neighbor pairing interactions, g_3 is the dominant mechanism determining the rise of T_c with the number of layers.

The authors thank J.G. Bednorz, K.A. Müller, A. Baratoff and S. Ciraci for stimulating discussions.

Appendix A

We consider the Hamiltonian $\mathcal{H}=\mathcal{H}_1+\mathcal{H}_2$ where $\mathcal{H}_1$ and $\mathcal{H}_2$ are given by Eqs. (20) and (5), respectively. We diagonalize $\mathcal{H}_1$ and $\mathcal{H}_2$ by the Fourier sine transform with respect to the z-direction

$$c_{\mathbf{k},l,\sigma}=\sqrt{\frac{2}{L_z+1}}\sum_{q=1}^{L_z}\sin\frac{\pi lq}{L_z+1}c_{\mathbf{k},q,\sigma}. \tag{A.1}$$

This results in

$$\mathcal{H}_1=\sum_{\mathbf{k},q,\sigma}(\tilde{\varepsilon}(\mathbf{k},q)-\mu)c^+_{\mathbf{k},q,\sigma}c_{\mathbf{k},q,\sigma} \tag{A.2}$$

and

$$\mathcal{H}_2=\frac{4}{L^2(L_z+1)^2}\sum_l\sum_{\{q_i\}}\sum_{\{\mathbf{k}_i\}}[g_0S_{q_1,l}S_{q_2,l}S_{q_3,l}S_{q_4,l}$$
$$+2g_3C_{q_1,1}C_{q_3,1}S_{q_1,l}S_{q_2,l}S_{q_3,l}S_{q_4,l}$$
$$+2g_3S_{q_1,1}S_{q_3,1}C_{q_1,l}S_{q_2,l}C_{q_3,l}S_{q_4,l}]$$
$$\cdot c^+_{\mathbf{k}_1+\mathbf{k}_3,q_1,\uparrow}c^+_{-\mathbf{k}_2-\mathbf{k}_3,q_3,\downarrow}c_{-\mathbf{k}_2,q_4,\downarrow}c_{\mathbf{k}_1,q_2,\uparrow}, \tag{A.3}$$

where $S_{q,l}=\sin[\pi ql/(L_z+1)]$ and $C_{q,l}=\cos[\pi ql/(L_z+1)]$.

To derive the gap equation we invoke the variational principle (6) and evaluate the right-hand side of (6) with respect to a trial Hamiltonian of the form (22). To calculate F_0 and $\langle \mathscr{H} - \mathscr{H}_0 \rangle_0$, we first diagonalize $\mathscr{H}_0$ by means of a Bogoliubov transformation. We minimize the right-hand side of (6) to obtain gap equation (23). Thereby use is made of the identities

$$\sum_{l=1}^{L_z} \sin^2 \frac{\pi q l}{L_z+1} \sin^2 \frac{\pi q' l}{L_z+1} = \frac{1}{4}(L_z+1) \cdot (1 + \tfrac{1}{2}\delta_{q,q'} + \tfrac{1}{2}\delta_{q+q',L_z+1}), \tag{A.4}$$

$$\sum_{l=1}^{L_z} \sin^2 \frac{\pi q l}{L_z+1} = \frac{1}{2}(L_z+1). \tag{A.5}$$

Linearization of gap equation (23) leads to

$$\Delta(q) = -\frac{1}{2(L_z+1)}\left(g_0 + 2g_3 \cos\frac{2\pi q}{L_z+1}\right) \cdot [\tilde{f}(q)\Delta(q) + \tilde{f}(L_z+1-q)\Delta(L_z+1-q)] - \frac{g_0+2g_3}{L_z+1}\sum_{q'} \tilde{f}(q')\Delta(q'), \tag{A.6}$$

where

$$\tilde{f}(q) = \frac{1}{L^2}\sum_{\mathbf{k}} \frac{1}{2\varepsilon(\mathbf{k}, q)} \tanh\left(\frac{\beta\varepsilon(\mathbf{k}, q)}{2}\right). \tag{A.7}$$

Equation (A.6) leads to a linear set of two equations for $\Delta(q)$ and $\Delta(L_z+1-q)$. Solving this set of equations we get

$$\Delta(q)\left[1 - \frac{1}{2(L_z+1)}\left(g_0 + 2g_3 \cos\frac{2\pi q}{L_z+1}\right)(\tilde{f}(q) + \tilde{f}(L_z+1-q))\right] = \frac{g_0+2g_3}{L_z+1}\sum_{q'} \tilde{f}(q')\Delta(q'). \tag{A.8}$$

As the right-hand side of (A.8) does not depend on q, (A.8) can be solved by making the ansatz

$$\Delta(q) = \frac{\Delta}{1 - \left(g_0 + 2g_3 \cos\frac{2\pi q}{L_z+1}\right)[\tilde{f}(q) + \tilde{f}(L_z+1-q)]/2(L_z+1)}. \tag{A.9}$$

Substitution of this expression for $\Delta(q)$ in (A.8) leads to (28) for T_c.

References

1. Strongin, M., Hammerer, O.F., Douglass, D.H., Cohen, M.H.: Phys. Rev. Lett. **19**, 121 (1967)
2. Frindt, R.F.: Phys. Rev. Lett. **28**, 299 (1972)
3. Fischer, Ø., Triscone, J.-M., Antognazza, L., Brunner, O., Kent, A.D., Mieville, L., Karkut, M.: Peprint
4. Li, Q., Xi, X.X., Wu, X.D., Inam, A., Vadlamannati, S., McLean, W.L., Venkatesan, T., Ramesh, R., Hwang, D.M., Martinez, J.A., Nazar, L.: Phys. Rev. Lett. **64**, 3086 (1990)
5. Lowndes, D.H., Norton, D.P., Budai, J.D.: Phys. Rev. Lett. **65**, 1160 (1990)
6. Schneider, T., Gedik, Z., Ciraci, S.: Europhys. Lett. **14**, 261 (1991)
7. Allan, G.A.T.: Phys. Rev. B**1**, 352 (1970)
8. Capehart, T.W., Fisher, M.E.: Phys. Rev. B**13**, 5021 (1976)
9. Ritchie, D.S., Fisher, M.E.: Phys. Rev. B**7**, 480 (1973)
10. Parga, N., Van Himbergen, J.E.: Ann. Phys. (NY) **134**, 286 (1981)
11. Chester, G.V., Fisher, M.E., Mermin, N.D.: Phys. Rev. **185**, 760 (1969)
12. Lawrence, W.E., Doniach, S.: In: Kanda, E. (ed.) Proceedings of the 12th International Conference on Low Temperature Physics, p. 361. Academic Press of Japan 1971
13. Pickett, W.E.: Rev. Mod. Phys. **61**, 433 (1989)
14. Schneider, T., Frick, M.: In: Müller, K.A., Bednorz, J.G. (eds.) Earlier and recent aspects of superconductivity. Springer Series of Solid-State Sciences, Vol. 90, p. 501. Berlin Heidelberg New York: Springer 1990
15. Deutscher, G., Müller, K.A.: Phys. Rev. Lett. **59**, 1745 (1987)
16. Bulaevski, L.N., Zyskin, M.V.: Preprint
17. Frick, M., Schneider, T.: Z. Phys. B – Condensed Matter **78**, 159 (1990)
18. Schneider, T., De Raedt, H., Frick, M.: Z. Phys. B – Condensed Matter **76**, 3 (1989)